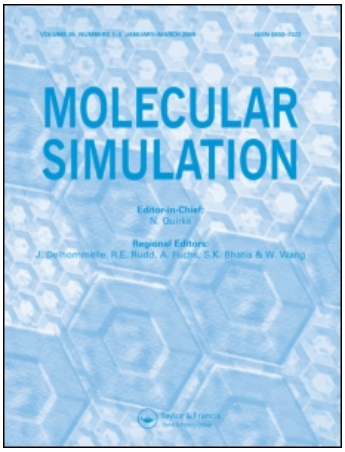

Molecular Simulation
Publication details, including instructions for authors and subscription information:
http://www.informaworld.com/smpp/title~content=t713644482

Novel Approaches to Cross-linking High Molecular Weight Polysaccharides: Application to Guar-based Hydraulic Fracturing Fluids

Peter V. Coveney[a]; Harshani de Silva[b]; Arthur Gomtsyan[c]; Andrew Whiting[b]; Edo S. Boek[d]
[a] Centre for Computational Science, Department of Chemistry, Queen Mary and Westfield College, London, E1, UK [b] Department of Chemistry, Faraday Building U.M.I.S.T., Manchester, M60, UK [c] Abbott Laboratories, Neuroscience Research D4PM, Abbott Park, IL, USA [d] Schlumberger Cambridge Research, Cambridge, CB3 OEL, UK

To cite this Article Coveney, Peter V. , de Silva, Harshani , Gomtsyan, Arthur , Whiting, Andrew and Boek, Edo S.(2000) 'Novel Approaches to Cross-linking High Molecular Weight Polysaccharides: Application to Guar-based Hydraulic Fracturing Fluids', Molecular Simulation, 25: 5, 265 — 299
To link to this Article: DOI: 10.1080/08927020008024503
URL: http://dx.doi.org/10.1080/08927020008024503

Molecular Simulation, 2000, Vol. 25, pp. 265–299
Reprints available directly from the publisher
Photocopying permitted by license only

NOVEL APPROACHES TO CROSS-LINKING HIGH MOLECULAR WEIGHT POLYSACCHARIDES: APPLICATION TO GUAR-BASED HYDRAULIC FRACTURING FLUIDS

PETER V. COVENEY[a,*], HARSHANI DE SILVA[b], ARTHUR GOMTSYAN[c], ANDREW WHITING[b] and EDO S. BOEK[d]

[a]*Centre for Computational Science, Department of Chemistry, Queen Mary and Westfield College, London E1 4NS, UK;*
[b]*Department of Chemistry, Faraday Building U.M.I.S.T., P.O. Box 88, Manchester M60 1QD, UK;*
[c]*Abbott Laboratories, Neuroscience Research D4PM, AP10/L-12E 100 Abbott Park Road Abbott Park, IL 60064-3500, USA;*
[d]*Schlumberger Cambridge Research, High Cross, Madingley Road, Cambridge CB3 OEL, UK*

(Received October 1999; accepted November 1999)

We report on recent work carried out using computational chemistry techniques which is aimed at suggesting novel ways of improving upon current methods of handling guar-based fracturing fluids. We describe generic methods available for modelling macromolecular, polysaccharide systems and apply these methods to building representative sections of the guar polysaccharide molecule, and to study its conformations *in vacuo* and in aqueous solutions using molecular dynamics. We then propose some novel cross-linking agents which differ from most of those currently under consideration in that they are extended, linear molecules related to polyethers. Representative cross-linking agents are then prepared and tested with various guar preparations. This study shows that with the correct choice of cross-linking agent, the overlap concentration C^* can be reduced below the expected level for particular guars.

Keywords: Polysaccharides; guar; cross-link agents; overlap concentration

*Corresponding author.

1. INTRODUCTION

Fracturing (frac) fluids are used to initiate and propagate rock fractures during oilfield hydraulic fracturing treatments. Commonly used frac fluids are based on guar gums and their derivatives. Various rheological properties of formulations, such as viscosity, are of great importance as these have to be at optimal levels to ensure that the fracture propagates correctly; if the viscosity is too low then fracture may not occur, whilst if the viscosity is too high then the friction pressure increases, resulting in high pumping costs. It is important to ensure that viscosity is retained under normal operating conditions, as guars tend to thin with increasing temperature. Cross-linking agents are deployed to produce highly viscoelastic gels that can carry small proppant particles into the fractures as they are formed. The proppant particles maintain the fracture open when the pumping pressure is extinguished. Cross-linking is particularly desirable in order to achieve good frac-fluid performance at low polymer concentrations. The cross-linking agents are usually small molecules or ions based on borates, titanates and zirconates. Cross-linking with these substances can either be made to occur immediately upon mixing, or it can be delayed by thermal and/or chemical means until the fluid is downhole.

When the proppant particles are in place, it is usually necessary to remove the cross-linked gel which would otherwise severely reduce the permeability of the fracture. To ensure that this is done effectively, so-called 'breakers' are added to the fluid, which break down the polymer gel network, usually in an indiscriminate and somewhat random way. The most widely used are oxidative breakers, such as peroxydisulphate ions. The guar polymer is attacked by free radicals formed when peroxydisulphate decomposes thermally at elevated temperatures. One advantage of using this particular oxidising agent is that very little is required to lower the viscosity of the gel. (Enzyme breakers can also be used, although they require more stringent conditions for successful operation: in the case of hemicellulase, for example, a pH of 3.5–8.0 and a temperature less than 65°C are needed in order for the enzyme to degrade the polymer.) The result is polymer residues of comparatively low molecular mass, with a concomitant dramatic decrease in the fluid viscosity. In this way, a high permeability route is found for the oil to flow towards the wellbore. However, when inorganic breakers are used the residues produced are often hydrophobic (since many of the hydrophilic galactose side groups shown in Fig. 1 are removed), and these tend to precipitate, hence reducing fracture permeability. Proposals have

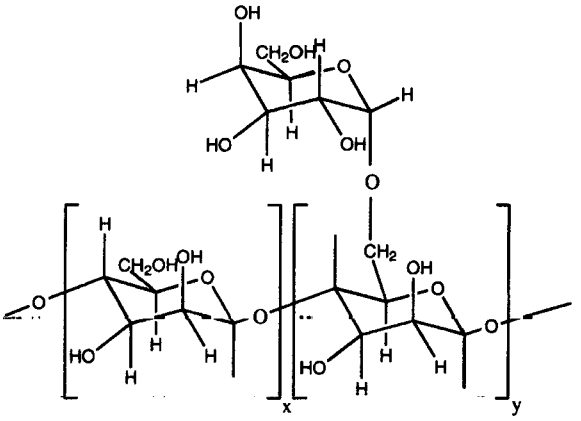

FIGURE 1 The repeat units in the molecular structure of guar showing the mannose backbone and random pendant galactose sidegroups; x and y denote the relative amount of galactose substitution.

been made to deal with this problem using surfactants which can solubilise these residues within micelles [1]. An additional point concerns clay/shale swelling which occurs when water-based fluids are used, as in drilling operations. Currently, KCl is added in high concentration (ca. 2 M) to inhibit swelling, but for environmental and other commercial reasons is currently deemed unacceptable. One would like to find cheap additives with the desired inhibitory properties that could be included in a frac fluid formulation.

In this paper, our main subject of study is the guar macromolecule and its interactions with various cross-linking molecules, some of which are based on borate chemistry while others are entirely novel in this context. Although the only polysaccharide we shall study here is guar, the principles and general conclusions also apply to related macromolecules, such as hydroxypropyl guar. The approach taken is a theoretical one based on a range of techniques drawn from state-of-the-art computational chemistry. The central idea behind this work is a very simple one: to lower the value of the polymer concentration needed for gel formation (the so-called overlap concentration C^* defining the semi-dilute régime in polymer physics [2]) through the design of extended cross-linker species. We then report synthetic studies, including the preparation of some of the new cross-linking agents and their effects, under various conditions, on the gelation of different commercial guars.

2. METHODS AND RESULTS

2.1. Simulation Methods and Potential Models

The principal simulation technique employed was molecular dynamics (MD) [3] as we were mainly interested in performing conformational studies. (For an up-to-date review of established techniques for the computer simulation of polymers, see Ref. [4].) A key element in the successful implementation of MD is the selection of suitable atomistic interaction potentials for the system under investigation and this Section is dedicated to a discussion of these. Since we had no intention of constructing our own force field for use in guar systems alone, which would be at best a lengthy and tedious task, we first sought out potential models that would prove satisfactory. There are some dedicated saccharide and polysaccharide force fields now available in the literature, for example that implemented within the CHARMM biomacromolecular modelling package [5], yet even that would prove too restrictive for our purposes, since our own applications seek to combine such molecules with others which do not fit within the specification of this force field. From our previous work involving other systems in aqueous environments [6–8], the natural choice for us to make is to use a slightly modified Dreiding force field; the bulk properties of water are reasonably well modelled in this way [7], as are various experimentally observable properties of clay systems [7, 8].

The potential energy of a molecular system is expressed as a sum of bonded and non-bonded interactions. The bonded interactions include harmonic potentials for stretching and bending interactions [9]. The non-bonded interactions are pairwise additive and are described by Coulombic and Lennard–Jones [6–12] parameters (Eq. (1)):

$$V = \sum_{i,j} \left[\frac{q_i q_j}{r_{ij}} - D_{ij} \left\{ 2 \left(\frac{\sigma_{ij}}{r_{ij}} \right)^6 - \left(\frac{\sigma_{ij}}{r_{ij}} \right)^{12} \right\} \right] \tag{1}$$

The bonded and non-bonded parameters can be found in Ref. [9]. Our own modification to this force field, which has been discussed elsewhere [6], is to use the TIP3P electrostatic charges and geometry for describing the water molecules [10], while employing Dreiding for van der Waals and bonded parameters. We should point out, however, that strictly the TIP3P model is defined as a rigid model, that is there are no bond stretching or bending parameters specified. However, the codes we have used in this work do not allow constraint dynamics to be imposed [3], so we have used effectively

rigid bonds and angles by employing Dreiding parameters for stretching and bending for these intramolecular water motions, since these are suitably large. In all our MD simulations, an integration time step of 1 fs (one femtosecond) was chosen to capture high frequency hydrogen-atom bond vibrations.

It should be emphasised that there are serious limitations to the use of molecular dynamics. It is an exceedingly CPU intensive technique, particularly for simulations involving a large number of atoms, and only enables short time scale events to be probed effectively (typically of the order of up to 100 picoseconds). Even with the most advanced of contemporary computers, simulations on models comprising more than about 25,000 atoms are prohibitive. This means that as far as polymer modelling is concerned, we have to strike a balance between the size of the polymer fragment modelled and the length of time taken to perform MD simulations. This compromise enables us to define a 'representative' fragment as one which is both computationally tractable to study and which provides a good description of important polymer properties.

We note in passing that there are now alternative simulation methods available, which are considerably less computationally expensive. Whereas molecular dynamics includes accurate molecular detail but is difficult to use for obtaining macroscopic information, simulation methods such as lattice-gas automata or dissipative particle dynamics provide useful information from the mesoscopic to the macroscopic levels and are computationally much faster [11, 12]. The price to be paid for this is that the molecular detail is largely ignored.

2.2. The Guar Molecule and Accessible Conformations

Guar is a linear polysaccharide consisting of a D-mannose backbone and D-galactose side groups. It has one of the highest molecular masses of all naturally occurring water-soluble polymers, the average mass being in the range of one to two million. The galactose side chains are arranged randomly on the mannose backbone, with galactose appearing on two or three consecutive mannose units (see Fig. 1). The ratio of mannose to galactose is approximately 1.6, but this is subject to variations depending on the biological origins of the material.

In this section, we describe our study of the structure of guar, both *in vacuo* and in aqueous solution. As noted above, a compromise has to be struck between the size of the polymer chosen for modelling and the time needed to perform an MD simulation. A related problem is well known in

the field of molecular simulation, namely protein folding: given a primary sequence of amino acids that comprise a protein, one would like to be able to perform molecular dynamics in order to determine the stable tertiary structure which it adopts in aqueous solution. However, the timescale for protein folding is on the order of milliseconds, roughly nine orders of magnitude larger than timescales accessible for MD. There is no way that one can use MD to predict the three-dimensional structure of a protein using today's technology. The same is true for polysaccharides. For these reasons, we have studied much smaller fragments of the guar molecule, hoping in this way to get insights into its general structural properties.

For the foregoing reasons, we worked in the main with a fragment of guar of molecular mass ca. 15000, containing approximately two thousand atoms. Even with such a small fragment it took 48 CPU hours to simulate 20 picoseconds of molecular dynamics on an SGI R4400 processor. Attempts to simulate larger fragments, of molecular masses 65000 (8400 atoms) and 125000 (16300 atoms), proved to be beyond the bounds of acceptable simulation times, even using an R8000 processor on an SGI Power Challenge Array.

Three different polymers were built by varying the mannose : galactose ratio along the chain. Initially we made a guar polymer with a mannose to galactose ratio of 2 : 1 (*i.e.*, with $x = y$ in Fig. 1), as shown in Figure 2. We also made a model of the mannose backbone devoid of galactose (*i.e.*, with $y = 0$ in Fig. 1); the result is shown in Figure 3. The α-helix-like structure adopted in Figure 2 is due to the presence of the hydrophilic side chains – galactose – which support effective intramolecular hydrogen-bonding between units some distance apart along the chain. Energy minimisation using a simple gradient descent algorithm did not significantly alter the conformation in either case.

As naturally occurring guars often have a mannose to galactose ratio of around 1.6 : 1, with the galactose groups arranged randomly, we also built a polymer with these specifications, making use of Flory's rotational isomeric state theory [13]. The resulting structure is shown in Figure 4, which was again essentially unchanged on energy minimisation. There is clear evidence for the persistence of helical portions within the chain, associated with M : G ratios around 2 : 1, while other portions devoid of galactose side groups are more nearly linear, as found in the previous two simulations. (It is interesting to note that these latter linear portions of the chain are believed to be the sites prone to attack and fragmentation by certain enzymes in the hemicellulase class [14]. Thus, if we knew what the structure of the enzyme was, we might even be able to perform simulations of the guar fragment within the active site.)

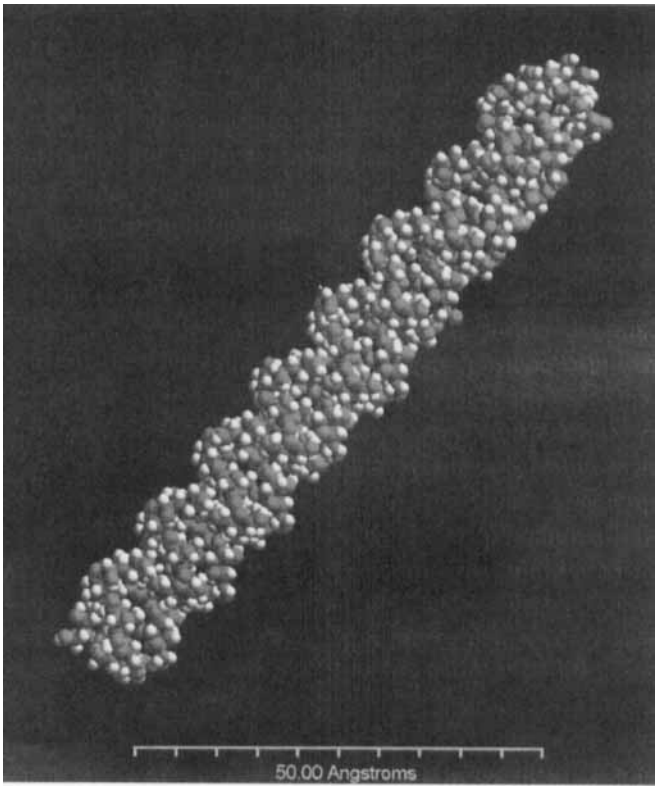

FIGURE 2 Structure of guar with a mannose : galactose ratio of 2 : 1.

In all, we constructed three such guar polymer fragments of differing molecular masses and, following energy minimisation, performed single-molecule molecular dynamics ('molecular mechanics') on these *in vacuo* for 20 ps, making use of the Nosé temperature-scaling MD algorithm within a canonical (NVT) ensemble at a temperature $T = 300$ K. The polymers were then analysed by calculating properties such as temporally-averaged radii of gyration and end-to-end distances from the trajectory files collected during the simulations. The results are tabulated in Table I. If desired, such data could be increased by performing a much larger number of simulations and then analysed to see how, for example, the radius of gyration R_g depends quantitatively on molecular mass.

From Table I, we can see that the trend is at least qualitatively in agreement with simple scaling theories, according to which $R_g \sim N^{\upsilon}$, where υ is an exponent that is 0.5 for ideal chains and 0.6 for self-avoiding random walk models. Some experimental data exist for related systems [15], though

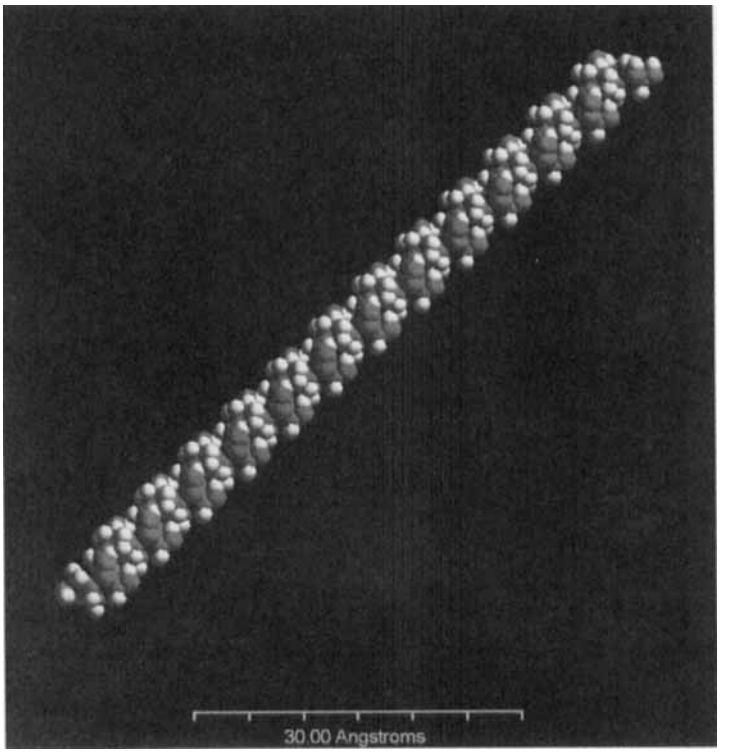

FIGURE 3 Structure of guar with a mannose : galactose ratio of 1 : 0.

from the point of view of the present article, there was no reason for us to carry out so many tedious and very lengthy simulations.

A more realistic study of guar than the *in vacuo* simulations described above has to take into account the polymer's aqueous environment in solution. To address this issue, we constructed three-dimensional simulation cells containing both water and polymer molecules. To represent an effectively infinite system, our simulation cell was initially constructed as a cube of side 30.7 Å with periodic boundary conditions applied in three dimensions. The cell dimensions were chosen to achieve aqueous guar solution densities of 1 g cm^{-3}; they contained a single guar fragment and a variable number of water molecules (as well as occasionally other ions). Polymers of chosen molecular mass may be constructed in this way in a wide variety of forms, including regular, random or block copolymers comprising a specified number of different monomers (which can themselves be arranged in regular or random intervals). A Monte-Carlo-like algorithm based on Flory's rotational isomeric state technique was used to build the

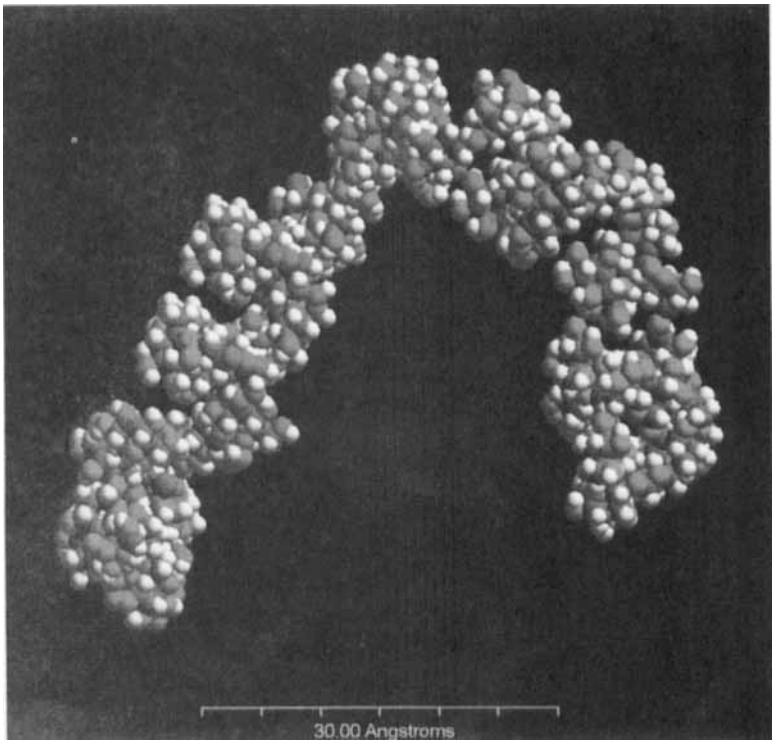

FIGURE 4 Structure of guar with a mannose:galactose ratio of 1.6:1.

TABLE I Some *in vacuo* properties of guar fragments of three different sizes

Property	*Small*	*Medium*	*Large*
Number of atoms	1955	8297	16000
Molecular mass/g mol^{-1}	15000	64000	125000
Radius of gyration/Å	13.81	26.90	62.57
End-to-end distance/Å	26.68	81.29	108.32

polymer in an energetically favourable conformation overall, in a similar way to that which generated the *in vacuo* fragment shown in Figure 4.

This polymer can then be inserted into a periodic simulation cell with a specified number of water molecules to achieve a chosen density. Molecular dynamics can be performed on this cell containing both polymer and water molecules, in order to provide information about conformations of the polymer and the concomitant structuring of water. In general, we performed all our MD simulations using the Nosé temperature-scaling algorithm in an isothermal-isobaric NPT-ensemble, with the temperature scaled at

$T = 300$ K and at a pressure of 1 atmosphere. The force field chosen for this work is that described above; a cut-off radius of 8.5 Å was imposed on the van der Waals interactions while Coulomb interactions were calculated using either the Ewald summation method or a simpler spline cut-off technique coming in at 8.0 Å and vanishing at 8.5 Å, the latter being used in most of the work described here as it is computationally much faster and did not produce significant discrepancies when compared to the more accurate Ewald sum. The coordinates of all the atoms in the cell were stored during an MD simulation for subsequent analysis as mentioned above. In the present context, the radial distribution function produces spherically-averaged distributions of inter-atomic vector lengths for selected atoms within the simulation cell (and its periodic images) and proves useful for determining structural properties such as conformations and packing of atoms, the ordering of solvent molecules around solutes, and detecting phase transitions.

As a simple check on the validity of the force field described above, we first performed MD simulations of (i) a cell containing 128 water molecules [6] and (ii) the disaccharide called α,α-trehalose (see Fig. 5) in a simulation cell together with 128 water molecules. This molecule has been the subject of a previous MD study [16] using more refined saccharide force fields and our results may be compared with those.

In addition, we performed molecular dynamics on a simulation cell containing a guar fragment and 128 water molecules; see Figure 6. A typical simulation, comprising 21.3 ps of MD performed on a guar fragment of molecular mass 15000, produced a temporally-averaged radius of gyration

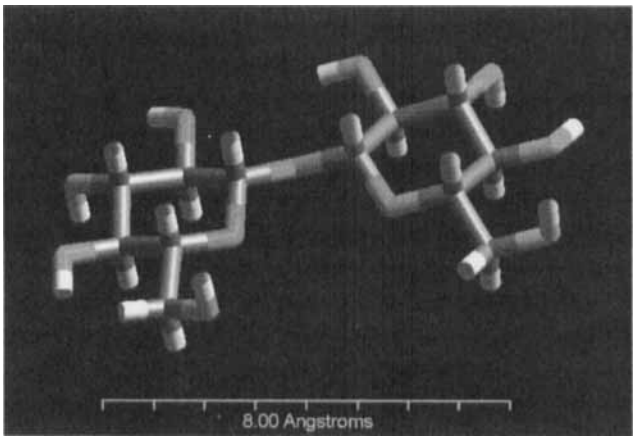

FIGURE 5 The trehalose disaccharide.

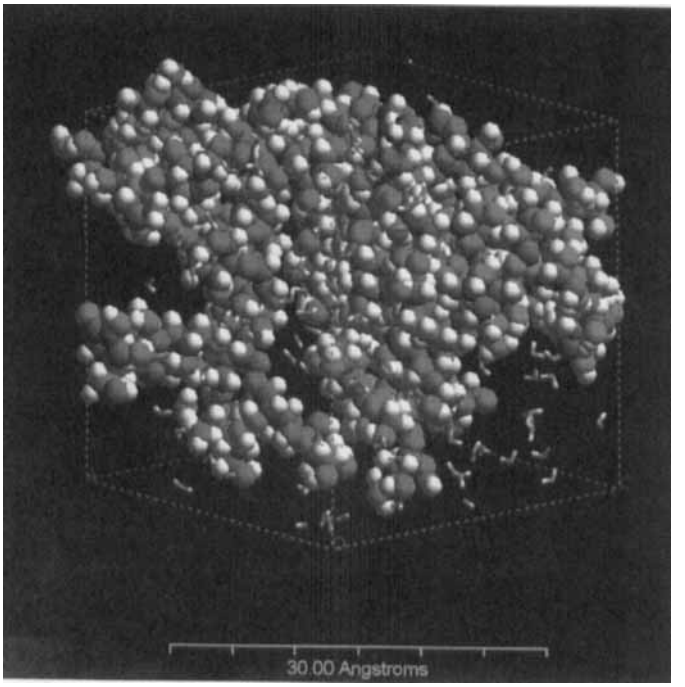

FIGURE 6 The periodic cell used in our molecular dynamics simulations.

of 15.47 Å and a temporally-averaged end-to-end distance of 19.17 Å. Figure 7 shows the radial distribution function of the oxygen atoms on the water molecules. The green curve represents the polysaccharide in water, the red represents the disaccharide in water and the blue plot shows the water alone in a cell. The first peak at small values of r is characteristic of the first neighbouring water shell; the structuring of the first water shell is reflected in the height and sharpness of the peak. It is evident that water alone displays a broad and low first peak, due to the comparative disorganisation in the packing of water molecules around one another; for the guar/water system there is a much narrower and higher peak, indicating that the water around the polymer is more ordered, while the structuring caused by the disaccharide is intermediate between the guar/water and water systems, as reflected by intermediate peak characteristics. The location of the first peak in the radial distribution function for our simulations of trehalose agrees well with that found by Pezron [15] providing some support for the use of our own chosen potential model.

Evidently, from our simulation work on small fragments, we would expect the full guar structure to approximate to some extent that of a

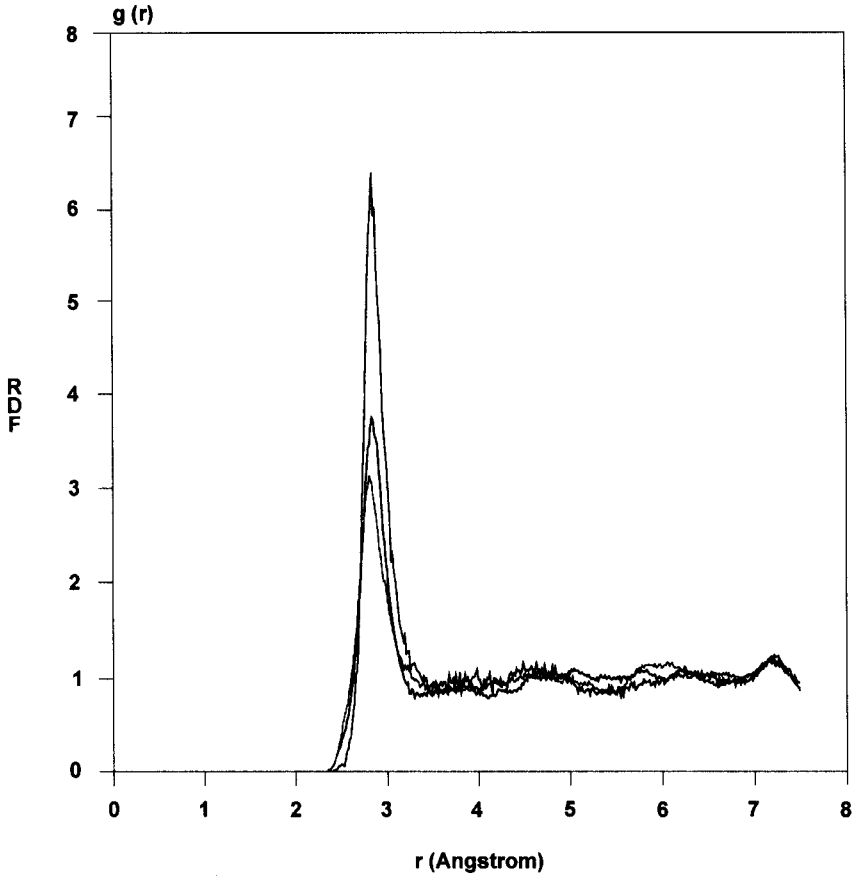

FIGURE 7 O–O radial distribution functions of oxygen atoms on water molecules in three simulations. (i) water (blue); (ii) water and trehalose (red); (iii) guar and water (green). (See Color Plate I).

random coil, with a persistence length estimated from Figure 4 of about 26 Å. By the term persistence length is meant the characteristic length along the chain over which the directional time correlation between individual segments disappears; loosely, it is the length over which a section of the chain is effectively rigid. According to Robinson *et al.* [17], the intrinsic stiffness of guar, as measured by the "characteristic ratio" for chain flexibility, C_∞, has the value 12.6. This value is based on a random flight model of a linear polymer in dilute solution, in which the chain is considered as a collection of stiff rods of length l connected by totally flexible, universal joints. These authors chose for l the value 5.4 Å, presumably on the basis that this corresponds to the length of a single mannose unit on the guar

backbone. Our models of guar have mannose monomer units of length 5.47 Å, confirming the interpretation of Robinson *et al.* The persistence length q was derived by these authors from the relation $q = C_\infty l/2$ and determined to have the numerical value of 34 Å, in at least qualitative agreement with that estimated by us. As we have seen, according to standard principles of polymer physics, a polymer comprised of more than about eight such consecutive lengths is deemed to be a random coil.

In reality, guar is certainly too flexible to be regarded as a rigid rod, but it may also be too rigid to be regarded as a fully random coil, as a result of intramolecular hydrogen bonding which provides a helical structure along those parts of the mannose backbone having a regular (2 : 1) M : G ratio (see Figs. 2 and 4); in particular, there are three repeat units of the form shown in Figure 1 (with $x = y = 1$) per turn of the helix. Nevertheless, for the purposes of this paper, it will suffice if we think of guar as essentially a random coil, in the spirit of Robinson *et al.* [17].

A limited study of the effects of ionic strength on the conformation of guar fragments was also carried out. In these simulations, we inserted ten sodium cations and ten hydroxide anions into the same periodic simulation cell, making use of the same Dreiding/TIP3P force field (which also supplies parameters for the Na^+ ion) in order to determine if there was any measurable effect on polymer properties. In these simulations, we used the same techniques as previously described to handle the coulomb interactions. A typical simulation, comprising 27.5 ps of MD performed on a guar fragment of molecular mass 15000, produced a temporally-averaged radius of gyration of 15.28 Å and a temporally-averaged end-to-end distance of 16.89 Å. Perhaps surprisingly, these values are little changed from those computed in the absence of the cations. It is possible that more extensive studies might have revealed more significant conformational changes in the polymer, as well as structural changes in the ionic and water environments, but limitations of time have prevented us from pursuing this further in the current work. However, it is known that the viscosity of non-ionic polymers such as guar and hydroxypropyl guar is only marginally affected by the presence of even high concentrations of monovalent salts. There is far less tolerance to multivalent cations – guar can become insoluble and precipitate if the concentrations of such salts are high enough.

2.3. The Effect of Cross-linking Agents

A single guar molecule contains a great many hydroxyl groups through which cross-linking may occur (mainly through the formation of

6-membered rings), so there is a finite probability that any single cross-linking molecule will be wasted by binding to hydroxyl groups within the same macromolecule. Conventionally, boric acid and borate salts are often used as cross-linkers for guar. The active species is the $B(OH)_4^-$ ion, which is formed at high pH's (Eq. (2)).

$$H_3BO_3 + OH^- \rightleftharpoons B(OH)_4^- \tag{2}$$

At a pH of 9–10 the gel formed is stable. (Evidently, the rate of cross-linking is itself important in frac fluid applications, since this controls the rheological properties of the fluid during pumping.) The viscosity of the gel formed decreases with increasing temperature as the cross-link density decreases, but the network structure reforms when the temperature is lowered. Titanate and zirconate based gels have different properties to borate-based gels, reflecting the different nature of the cross-linking in these cases. Typically, the metal-ion based gels are more thermally stable than the borate-based gels and do not recover their viscosity after undergoing shear: this can be understood, albeit somewhat tautologically, in terms of the effective irreversibility of cross-linking in the case of titanates and zirconates; the borate-guar cross-links are, by contrast, essentially reversible and the equilibrium constants strongly temperature-dependent.

In order to overcome the problem of intramolecular cross-linking, while simultaneously encouraging the possibility of intermolecular cross-linking at guar concentrations appreciably below C^*, we propose in this section a set of novel molecules. From the foregoing requirements, such molecules should ideally be rigid-rod-like, with guar-binding capability at both ends. Thus the issues that we must address concern the specification of the 'rigid' backbone and the nature of possible functional groups. An obvious but important constraint on the molecule's properties is that it be soluble in water. A natural choice for the basic structure we seek is based on the polyethers. These have a structure which can be made more or less hydrophilic by suitable arrangement of substituents along the chain; at the same time, difunctionality is readily introduced at the two ends of the chain. Some potential benefits are immediately clear: molecules such as the polyethylene glycols (PEGs) are known to be effective shale-swelling inhibitors, and we already have extensive experience of performing molecular simulations with these [7]. Furthermore, by transferring our main investigations to these smaller molecules, we can achieve more useful and more accurate molecular dynamics results than for the guar macromolecule.

The basic philosophy advocated in the remainder of this paper finds support from two sources. One of these is recent work performed on the

cross-linking of tetrabutylammonium polygalacturonate with alkyl or alkylaryl dihalides in which the significance of different cross-linker chain lengths is assessed [22], although these studies were carried out at C*. The other originates in a Japanese patent which describes the production of viscous gels on mixing boronic acid copolymers (of typical mass 30000) and polyvinyl alcohols: these gels returned to sols on addition of glucose [18].

Our initial proposal is concerned with attaching borate groups to both ends of these diols, in an attempt to create extended cross-linkers through esterification of the hydroxyl groups on different guar molecules (mainly formed through six-membered cyclic esters on the galactose residues). The basic reaction producing the diborate species is represented in Figure 8 for the case of PEG300 and the cross-linked product is illustrated in Figure 9. Making use of our previous work on clay-swelling inhibitors, we began by studying the diborate derivative of PEG300 (that is, polyethylene glycol of molecular mass approximately 300 and chemical formula $[HO(CH_2\ CH_2O)_6]H$, *cf.* Fig. 8). We constructed this molecule in the same way as guar, by building it in a cell with a total of 128 water molecules, and at a density of $1\,g\ cm^{-3}$. NPT molecular dynamics was then performed for a total of 50 ps. In order to investigate the rigidity of the

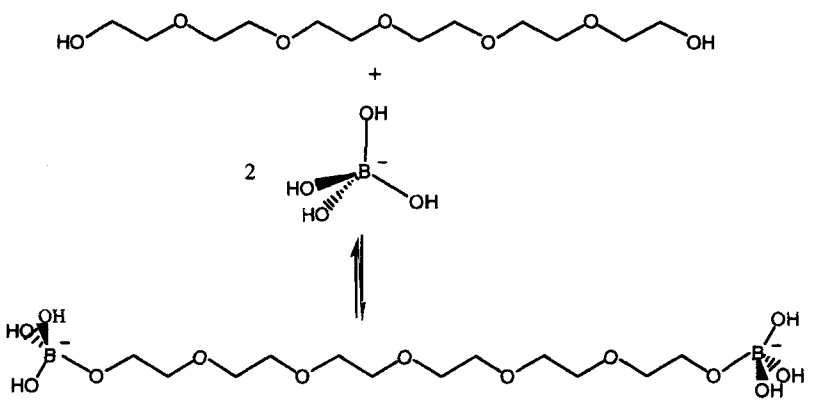

FIGURE 8 Production of a PEG-diborate anion starting from PEG300.

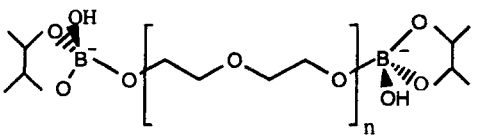

FIGURE 9 Mechanism for cross-linking with guar.

polyethylene backbone in the homologous series of PEGs, we also studied diborate derivatives of PEG600 ($[HO(CH_2CH_2O)_{12}]H$) and PEG10000 ($[HO(CH_2\ CH_2O)_{150}]H$) using the same methods; Figure 10 shows a typical periodic simulation cell containing an aqueous solution of PEG600 diborate. Temporally averaged radii of gyration and snap-shot values of end-to-end distances for these species were computed from their MD trajectory files: these data are collected in Table II.

The persistence length in these PEG diborates is roughly 6 Å, as estimated by direct inspection of our simulation results. This estimate, which is quite a conservative one, is equivalent to a sequence of approximately four monomer units in length [19], *i.e.* $(CH_2CH_2O)_4$. Thus, according to simple principles of polymer physics, beyond a distance of roughly 32 Å (eight

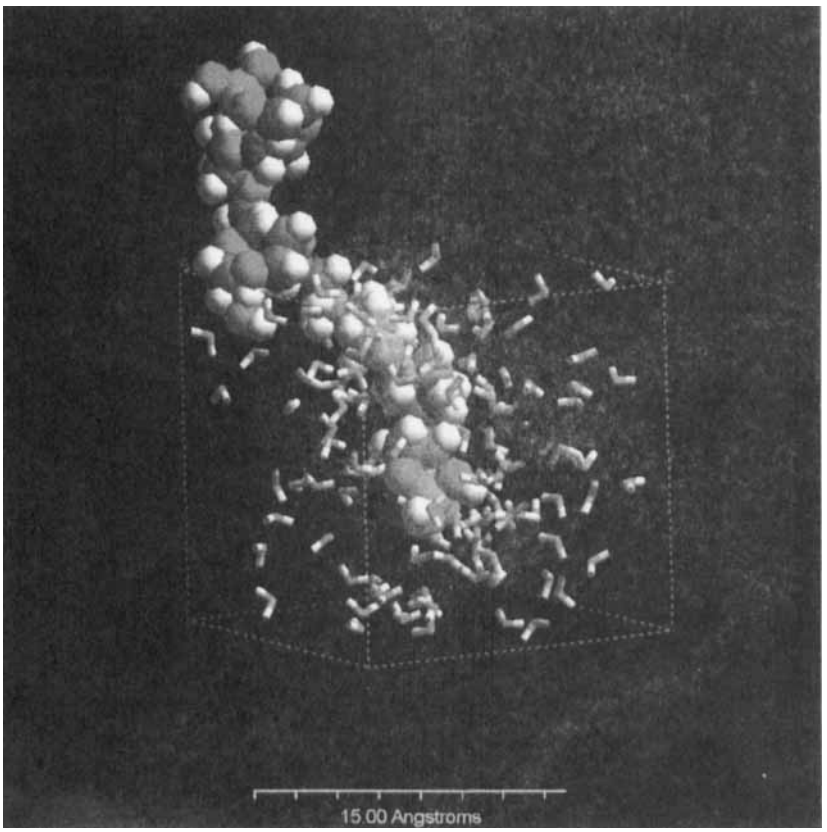

FIGURE 10 Periodic simulation cell (blue dotted lines) containing PEG600 diborate in an aqueous environment. (See Color Plate II).

TABLE II Properties of various polyether diborate cross-linkers in aqueous solution

Organic fragment between borate groups	*Molecular weight of cross-linkers/g mol*$^{-1}$	*Radius of gyration/Å*	*End-to-end distance/Å*
PEG300	300	8.18	9.79
PEG600	600	9.37	21.31
PEG10000	10000	23.67	17.96

times the persistence length), a PEG cross-linker behaves like a random coil. In terms of polyethylene groups, this is equivalent to a polyethylene unit of length $(CH_2CH_2O)_{32}$. Having random-coil cross-linkers would not be very effective if the guar needs to be cross-linked below C*. Note again that while in principle MD could be used to investigate dynamical scaling behaviour of such polymers in solution, it is computationally very intensive and relaxation behaviour has only recently been studied for model chains [20]. A more computationally efficient procedure is to draw on dissipative particle dynamics [21].

The borate scenario which we have described here seems to be promising. However, there is one important problem which must be addressed. If the borate cross-linker is produced *in situ* by mixing the PEG, guar and borate anions in aqueous solution, then with overwhelming probability the borate groups will migrate to the hydroxyl-rich guar surface and cause intramolecular cross-linking – the very result which we are trying to avoid. There are a number of ways of avoiding this, at least in principle. One of these would be to prepare the PEG-diborate species separately from the guar solution, and mix the two together at the appropriate moment; however, this is likely to be impractical for various reasons, *e.g.*, the difficulty of mixing reagents downhole, the likelihood that the diborate species only exists in equilibrium together with significant concentrations of the diol and simple borate anions which would then link intramolecularly, and so on.

One way to eliminate some of these difficulties is to modify the chemical structure of the cross-linker species slightly. For example, one could use PEG diboronate species, in which the boron atoms are attached directly to carbon atoms in the rod-like cross-linking chain, as illustrated in Figure 11, instead of diborates. Such molecules could be synthesised readily (*vide infra*), and would obviate the need to use borate as a separate additive. Grand canonical Monte Carlo simulations following the method used in our clay simulation studies [7] indicate that these molecules may be effective clay swelling inhibitors, at least in their neutral form; a simulation snap-shot is shown in Figure 12.

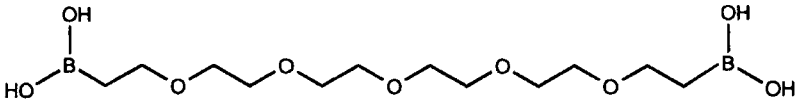

FIGURE 11 PEG300 diboronate.

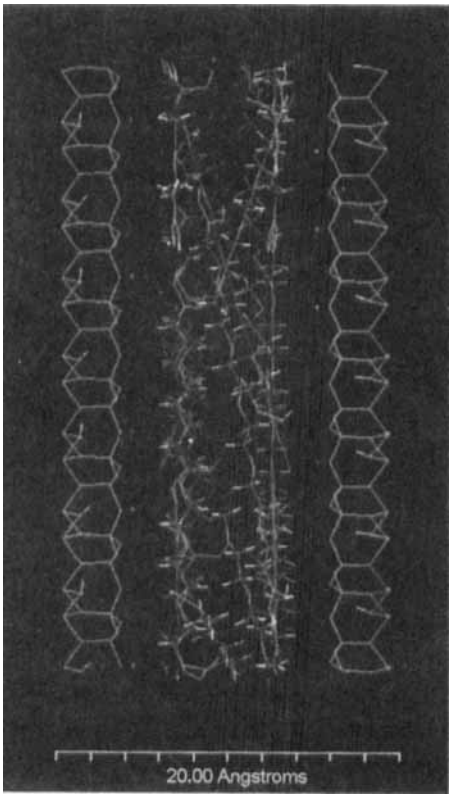

FIGURE 12 PEG300 diboronic acid sorbed into a sodium montmorillonite clay – grand canonical Monte Carlo simulation.

Other extended cross-linkers that could be constructed are those with aldehyde (or possibly bromide or iodide) functionality at each end rather than borate (see Fig. 13). These molecules, whose conformations are similar to those of the diols described above, would cross-link by a kind of condensation reaction with hydroxyl groups on guar (Fig. 14); since no borate anions would be present, there would also be a much higher chance of delivering intermolecular as opposed to intramolecular links, as with the diboronates. Moreover, the diacetal so formed can be ruptured on

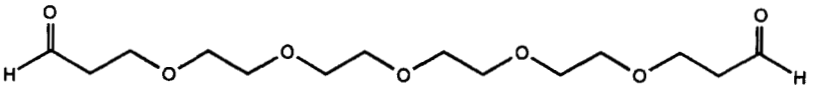

FIGURE 13 A dialdehyde molecule.

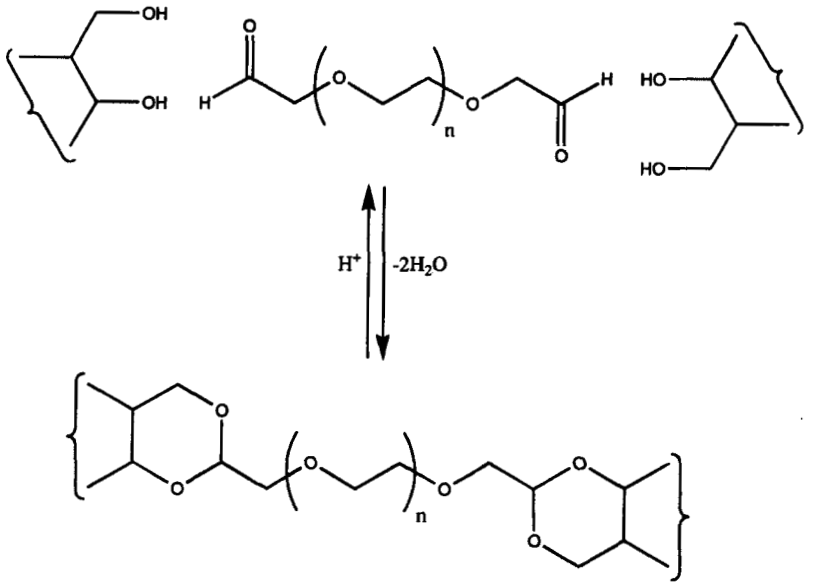

FIGURE 14 Mechanism of cross-linking of guar with a PEG dialdehyde.

acidification, thus breaking the cross-links. It seems likely, however, that the cross-linkers formed from such dialdehyde molecules would probably not break under shear (being in this sense more like the zirconate and titanate cross-linkers), whereas the PEG-diborate and PEG-diboronate cross-linkers would break (as is the case for the simpler borates). Finally, as with the diols (*vide supra*), these molecules should also act as shale-swelling inhibitors, according to the results of grand canonical Monte Carlo simulations which we have performed (see Fig. 15) these show similar behaviour to the diols and diboronates discussed above.

One point of detail is worth mentioning here: the accepted and well established mechanism for formation of an acetal from a diol involves a simultaneous protonation of the aldehyde oxygen as the alcohol adds to the carbon atom of the carbonyl group. It is thus an acid-catalysed reaction. However, the reaction does proceed under neutral conditions (at least for reactive aldehydes), the acidity of an alcohol (or water)

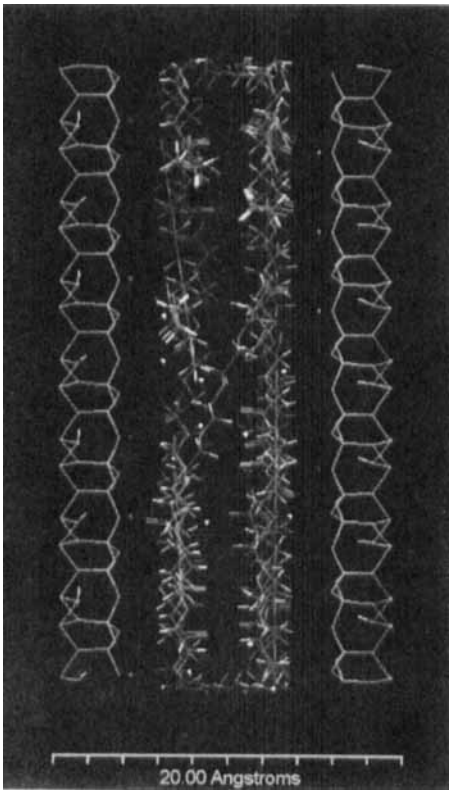

FIGURE 15 PEG300 dialdehyde sorbed onto sodium montmorillonite clay – grand canonical Monte Carlo simulation.

being sufficient. Certainly at pH 8–9, one would expect the alcohol functions on guar to be capable of reacting with an aldehyde. Possibly, the rate of acetal formation would go down as a function of increasing pH; this could be easily checked using n.m.r. spectroscopy. However, while an alkaline pH is required for borate cross-linking species, since only the anion can cross-link in the desired manner, for a dialdehyde one could happily perform cross-linking at lower pH's where reaction is known to proceed efficiently.

Another class of related molecules whose properties it is worth investigating are the so-called 'Pluronics', block copolymers comprising hydrophobic and hydrophilic portions. A much simplified Pluronic structure is displayed in Figure 16. The hydrophilic portions are generally

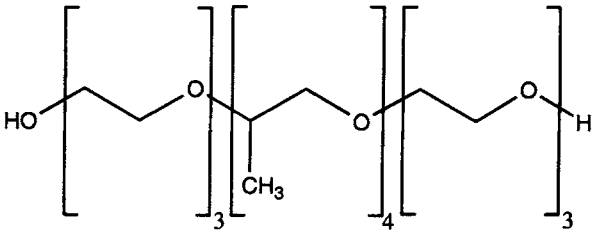

FIGURE 16 The simple EO/PO Pluronic diol used in our simulations.

ethylene oxide (EO) units, while the hydrophobic parts are typically comprised of propylene (or butylene) oxide (PO or BO) units. Because of this, at least certain of these have the capability to form micelles at sufficiently high concentrations, as indicated in Figure 17 [23].

The *in vacuo* structure of one such commercially available Pluronic molecule, $HO(CH_2CH_2O)_{27}(CHMeCH_2O)_{39}(CH_2CH_2O)_{27}H$, is shown in Figure 18. For reasons associated with CPU time, we did not do any simulation work using this particular molecule, however. Instead, simulations were performed with a greatly scaled down version of chemical formula $HO(CH_2CH_2O)_3(CHMeCH_2O)_4(CH_2CH_2O)_3H$ and molecular mass 514 (as shown in Fig. 16). For brevity, we shall henceforth refer to this small Pluronic as **A**.

Some computational work was performed in an attempt to see whether **A** might show any tendency to form micelles [24]. This was done by constructing a periodic simulation cell containing 10 Pluronic molecules **A** and 128 water molecules (at a density of 1 g cm^{-3}); molecular dynamics was then applied using the NPT method for 100 ps. However, it was difficult to draw any conclusions from this simulation as to whether micellisation had occurred either by direct visualisation or by examination of the C–C radial distribution function, which only gave peaks corresponding to characteristic intramolecular C–C distances. It is possible that the simulation did not run for a sufficiently long time or, perhaps, that for molecules of the small size used in our simulations, micelles would not actually form in any case.

These types of molecules generally behave in a chemically similar way to the polyether diols (*vide supra*). As in the case of the other molecules considered thus far, we would also expect them to be efficient clay-swelling inhibitors [7]. The novelty of micelle-forming Pluronics as potential cross-linkers of guar polymers is that, if they are run at concentrations

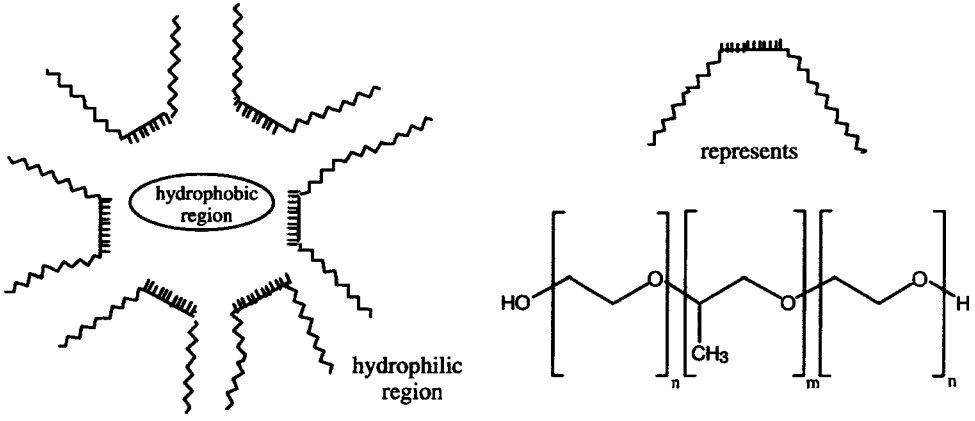

FIGURE 17 Micelle formation in a general Pluronic system.

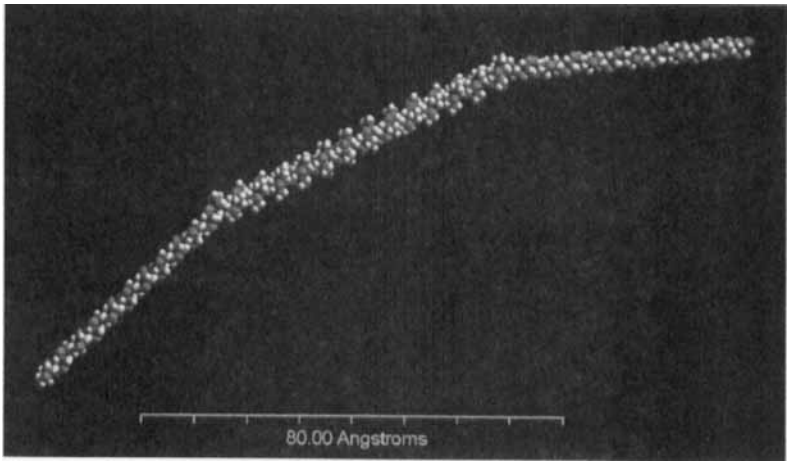

FIGURE 18 A typical commercially available Pluronic variant.

above their critical micelle concentrations, they may also prove effective at dissolving the insoluble mannose residues produced by oxidative breakers. Hitherto, this approach has been considered through the addition of specific surfactant species, typically based on quaternary ammonium ions.

2.4. Synthesis and Evaluation of New Cross-linking Agents

Having carried out extensive modelling of the guar system and of possible cross-linking agents, the synthesis and evaluation of new agents was undertaken. The aim of this part of the work was to carry out a study on the effect of various additives to different guar-based gels (*vide infra*). In particular, the aim was to determine whether it was possible to produce gels at a concentration of guar below what is currently believed to be the critical concentration C^*, which is defined for the guar used (J424) as 2.40 g of guar per litre of water. Of many potential target additives, compounds **1**–**5** were selected on the basis of ease of synthesis and to test the modelling work described above.

2.4.1. Preparation of Gel Additives

Compounds **1** and **4** were purchased from Aldrich and Shearwater respectively, and used directly. The remaining compounds were prepared

as outlined below (Scheme 1 and Eq. (1)).

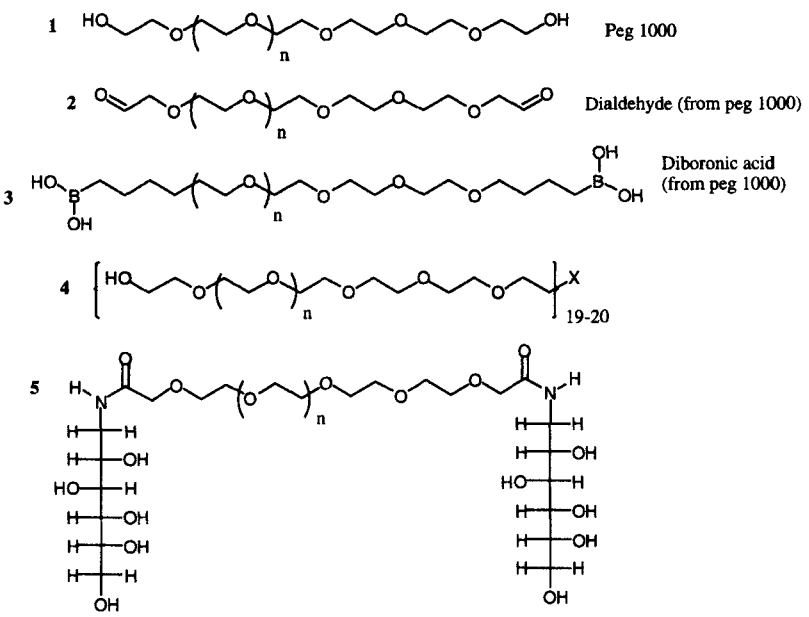

In order to prepare the dialdehyde **2** from diol **1**, Swern oxidation was efficiently applied to produce the required dialdehyde in 99% yield. To access diboronic acid **3**, we first had to introduce a terminal double bond in order to accomplish a hydroboration reaction to introduce the boronic acid moiety. This was achieved by a four stage process which involved double terminal bromination of diol **1** (Scheme 1) by a tosylation and bromine-tosyl exchange reaction. The resulting dibromide could then be reacted with allylmagnesium bromide and the intermediate terminal alkene hydroborated with borane-tetrahydrofuran complex. Final hydrolysis of the resulting borane *in situ* with dilute hydrochloric acid gave the double terminal boronic acid **3**, which was used directly for the gel preparations.

The final cross-linking agent synthesised was diglucamide **6**, which was prepared *via* commercially available diacid **6**. *In situ* chlorination of **6** was accomplished with thionyl chloride (Eq. (3)) and the resulting acid chloride was immediately transformed into the diglucamide **5** by reaction with commercially available glucamine in a mixture of tetrahydrofuran-water, buffered as necessary to keep the reaction at pH 8.

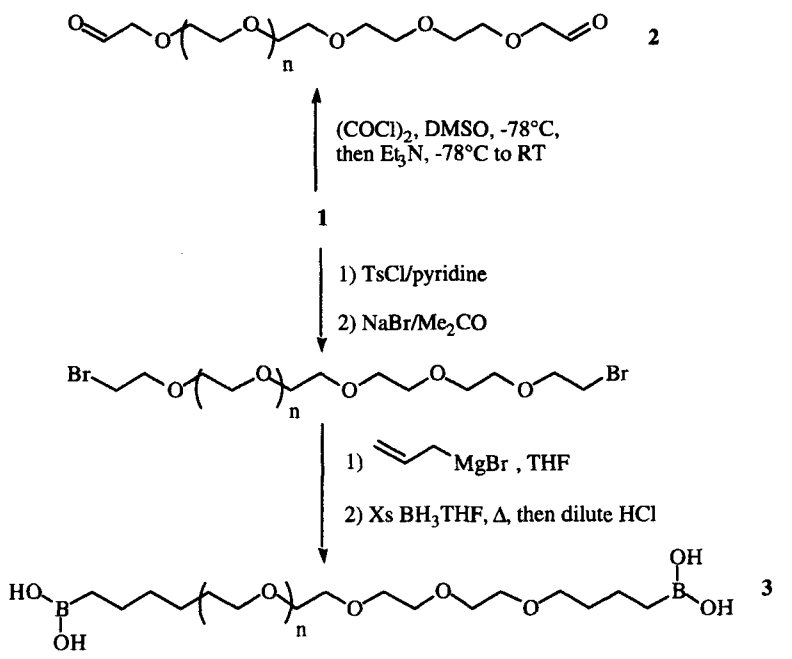

SCHEME 1 Synthetic scheme for the preparation of dialehyde and diboronic acid PEG analogues.

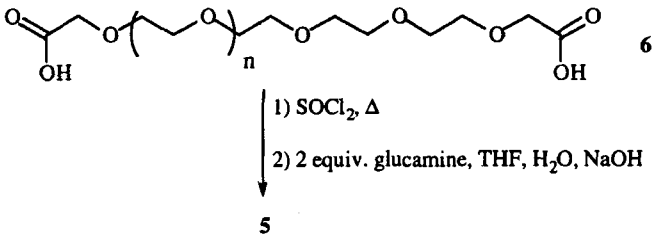

Preparation of PEG diglucamide.

2.5. Testing and Results of Gel Additives

For the purpose of testing the gels, guar solutions were prepared by vigorously mixing guar J424 with water, and leaving the solution to "hydrate" for 1.5 hours before use. The effect of adding the various additives (Tab. I) was ascertained by mixing the pre-hydrated guar, mixing thoroughly in a blender and pouring a sample into a 50 ml widemouth glass bottle. The resulting gel strengths were recorded using the bottle-test

gel-strength codes (see Tab. IV) and are shown in Table III and graphically for each guar concentration in Graphs 1 – 5.

Gel code key: 1 = A; 2 = B; 3 = C; 4 = D; 5 = E; 6 = F; 7 = G; 8 = H; 9 = I; 10 = J.

At a concentration of 4.8 g/l of guar, one would expect reasonable strength gels, whether additives are present or not. However, it can be seen from Graph 1 that in the absence of any cross-linking agent (Run 1), the resulting liquid is barely thicker than pure water. The effect of adding borate alone is remarkable, as long as the pH is kept basic (Run 9), producing one of the highest strength gels. However, similarly efficient is the gel resulting from addition of peg **1** and borate at basic pH (Run 7). It is noteworthy that

TABLE III Table showing the formulation used for each set of gel preparations and ensuing gel strength test results for J424 guar (see Tab. IV for the definition of gel strength codes)

Run	*KCl* (%)	*pH*	*Additive* 1(*g/l*)	*Boric acid* (*g/l*)	*Code* 4.8 *g/l Guar*	*Code* 3.6 *g/l Guar*	*Code* 2.4 *g/l C*Guar*	*Code* 2.1 *g/l Guar*	*Code* 1.8 *g/l Guar*
1	2	6–8	–	–	A	A	A	A	A
2	2	10	0.356 **1**	0.144	E	E	C	C	A
3	2	10	1.160 **1**	0.144	E	E	E	B	A
4	2	6	1.160 **1**	0.144	A	A	A	A	A
5a	–	10	2.320 **1**	0.288	F	F	E	D	C
5b (24 hours)	"	"	"	"	G	G	E	D	C
6	–	10	4.640 **1**	0.288	G	G	D	D	D
7a	–	10	2.320 **1**	0.288	F	F	E	C	C
7b (24 hours)	"	"	"	"	I	H	E	C	C
8a	–	10	4.640 **1**	0.288	F	F	E	C	C
8b (24 hours)	"	"	"	"	H	H	E	C	C
9	2	10	–	0.144	I	C	C	C	B
10	2	10	0.144 **2**	–	B	B	A	A	A
11	2	6	1.064 **2**	0.144	A	A	A	A	A
12	2	10	1.440 **2**	–	B	B	B	B	B
13	2	10	2.632 **3**	–	G	E	C	B	B
14	–	10	0.660 **5**	0.144	C	C	C	B	A
15a	–	10	1.320 **5**	0.144	C	C	C	B	A
15b (24 hours)	"	"	"	"	H	G	E	C	C
16	–	10	0.660 **5**	–	C	C	B	A	A
17	–	10	1.320 **5**	–	C	C	C	B	B
18a	–	10	1.320 **5**	0.288	G	F	E	E	E
18b (24 hours)	"	"	"	"	H	G	E	E	E
19	–	10	12.10 **4**	0.144	–	–	E	–	–
20	–	10	12.10 **4**	–	–	–	A	–	–
21	–	10	–	0.288	F	F	C	C	C
22	–	10	–	0.576	F	F	E	C	C

TABLE IV Definition of gel strength codes

Code	*Observation*	*Comment*
A	No detectable gel formed.	The gel appears to have the same viscosity (fluidity) as the original polymer solution and no gel can be visually detected.
B	High Flowing gel.	The gel appears to be only slightly more viscous than the initial relatively low-viscosity polymer solution.
C	Flowing gel.	Most of the detectable gel flows to the bottle cap upon inversion.
D	Moderately flowing gel.	A small portion (about 5–15%) of the gel does not readily flow to the bottle cap upon inversion – usually characterized as a "tonguing" gel (*i.e.*, after hanging out of the bottle, the gel can be made to flow back into the bottle by slowly turning the bottle upright).
E	Barely flowing gel.	The gel slowly flows to the bottle cap and/or a significant portion (greater than 15%) of the gel does not flow to the bottle cap upon inversion.
F	Highly deformable non-flowing gel.	The gel does not flow to the bottle cap upon inversion (gel flows to just short of the bottle cap).
G	Moderately deformable non-flowing gel.	The gel flows about halfway to the bottle cap upon inversion.
H	Slightly deformable non-flowing gel.	The gel surface only slightly deforms upon inversion.
I	Rigid gel.	There is no gel-surface deformation upon inversion.
J	Ringing rigid gel.	A tuning fork-like mechanical vibration can be felt after the bottle is tapped.

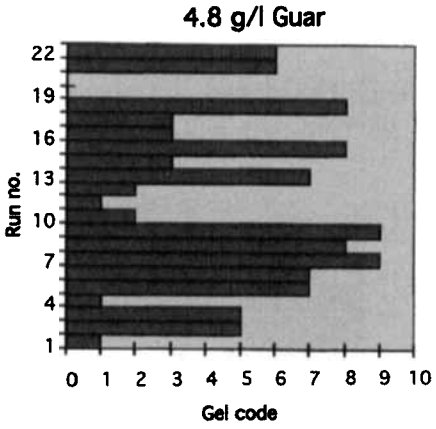

GRAPH 1 Additive effects on gel strength at 4.8 g/l guar.

this gel 'ages' over a 24 hour period to be as strong as gel 9 (see Tab. III, Run 7b). The essential effect of using a basic pH (ca. 10) is graphically shown by contrasting Runs 2 and 3 *versus* 4; Run 4 differs by being carried out at pH 6. This clearly indicates the importance of keeping the borate in

the form of an 'ate'-complex, thus validating the process shown in Figure 8. Identical effects are seen at all other guar concentrations (*vide infra*).

At a concentration of 3.6 g/l of guar, one would still expect reasonable strength gels, however we begin to observe a drop off in performance, with little difference between Runs 7 and 8, which include both diol **1** and borate. Run 8 contains twice the quantity of diol **1**; clearly above 2.320 g/l of diol makes little difference to the gel strength. However, below this quantity, performance is impaired, as indicated by Runs 2 and 3.

We can view a concentration of 2.4 g/l of guar as the most important guar concentration. If new effective gels cannot be produced at this concentration, the new additives would offer little advantage over established gel formulations. We can see from Graph 3 that, despite the expected drop off in performance, we still observe reasonable gels. Even more interesting however, is that fact that a variety of additives now start to show very similar behaviour, *i.e.*, Runs 3, 5, 7, 8, 15, 18, 19 and 22, which involve the addition of peg **1** (low concentration) and borate, peg **1** (medium concentration) and borate, peg **1** (high concentration) and borate, diglucamide **5** and borate (low concentration), diglucamide **5** and borate (high concentration), star peg **4** and borate, and borate alone (very high concentration, *i.e.*, twice that in Run 18 and four times that in Run 19). These results clearly show the useful synergistic effect of adding both alcohols and borate, *i.e.*, one can reduce substantially the borate required for reasonable gel performance.

At a concentration of 2.1 g/l of guar, the guar concentration has dropped below C*, *i.e.*, below the point at which we can expect gel formation at all.

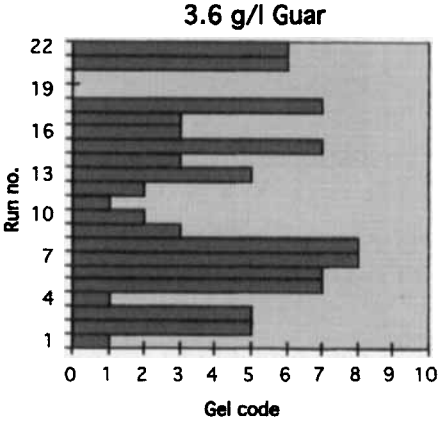

GRAPH 2 Additive effects on gel strength at 3.6 g/l guar.

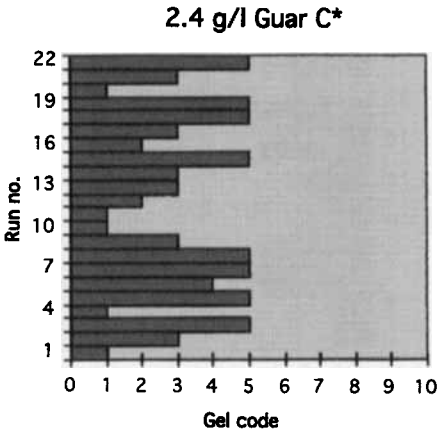

GRAPH 3 Additive effects on gel strength at 2.4 g/l guar.

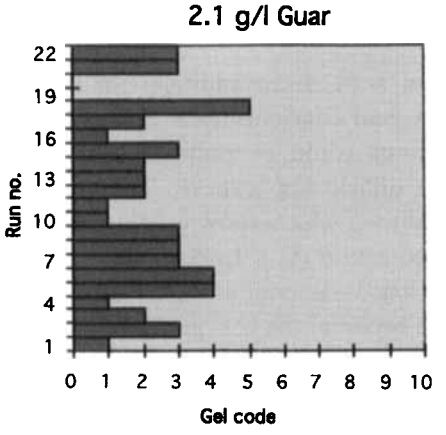

GRAPH 4 Additive effects on gel strength at 2.1 g/l guar.

However, we still observe gels being formed, with one outstanding gel which retains its performance from the higher concentration of 2.4 g/l of guar, *i.e.*, Run 18 which contains diglucamide **5** and borate. Thus, at this guar concentration, the diglucamide offers superior performance at lower guar concentrations.

At a concentration of 1.8 g/l of guar, one might expect no reasonable gel formation; however, as with the higher 2.1 g/l guar concentration, we see the very efficient effect of diglucamide **5**, Run 18, which still shows a gel strength of E – a remarkable result.

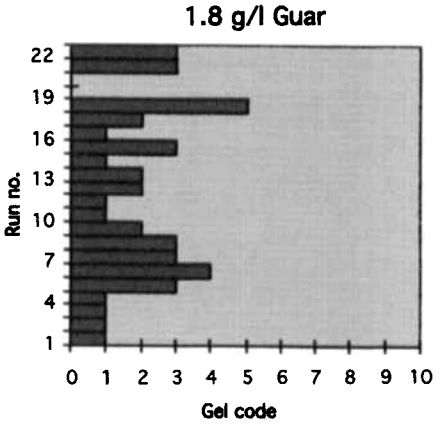

GRAPH 5 Additive effects on gel strength at 1.8 g/l guar.

3. CONCLUSIONS

We set out to design new, cheap additives for hydraulic frac-fluids that would operate at low guar concentrations. Such additives would mean that the guar concentrations could be reduced, which in turn would mean economic benefits in oilfield applications. The goals were realised by the design of specific additives which allow gel formation to occur even below the critical gel concentration (C^*). In particular, the addition of peg **1** to guar-borate preparations is superior at higher guar concentrations; however diglucamide **5**-borate becomes the best performer as the guar concentration drops below C^*. Our findings clearly demonstrate that: (a) it is indeed possible to form strong gels below C^*; (b) molecular modelling can assist in the design of new and multifunctional cross-linking agents.

Acknowledgements

We thank Chris Hall and Simon Ross-Murphy for helpful discussions during the development of this work.

APPENDIX: SUPPLEMENTARY MATERIAL: EXPERIMENTAL SECTION

For thin layer chromatography Merck [silica gel 60 F_{254} (Art. 5735)] or Macherey – Nagel [Sil G/UV_{254} (Art. 805201)] silica coated plastic sheets

were employed. Chromatograms were developed with either iodine vapour or a phosphomolybdic acid (10.0 g in 100 ml of ethanol or methanol) spray and with subsequent heating. For silica gel chromatography Merck Kieselgel H (Type 60) or Acros silica gel (0.035–0.07 mm) was used.

n-Butyllithium was purchased from Aldrich. Toluene and dichloromethane were dried by distillation from calcium hydride, and tetrahydrofuran was distilled from sodium-benzophenone ketyl immediately prior to use, and all distillations carried out under an atmosphere of argon. Light petroleum refers to the fraction boiling in the range 40–60°C. All anhydrous reactions were carried out in oven dried (140°C) glassware and cooled under a stream of argon. For rotary evaporation, a Büchi rotary evaporator or a Büchi cold finger rotary evaporator was used followed by evaporation under-high vacuum. Bulb to bulb distillation was achieved using a Büchi GKR-51 Kügelrohr distillation apparatus. Melting points were determined using an Electrothermal melting point apparatus and are uncorrected.

^{1}H and ^{13}C NMR were recorded at 300 and 75.6 MHz respectively on a Bruker AC300 NMR spectrometer, using $CDCl_3$ as a internal standard. ^{11}B NMR spectra were recorded at 64.2 MHz respectively, on a Bruker AC200 NMR spectrometer, relative to $BF_3 \cdot OEt_2$ in $CDCl_3$ as external standard.

Infrared spectra were recorded on a Perkin–Elmer 783, equipped with a PE600 data station, or a Perkin–Elmer 1600 Series FTIR. UV spectra were recorded on a Perkin–Elmer 115 spectrometer. Electron impact (EI) (70 eV) and chemical ionisation (CI) mass spectra were recorded on a Kratos MS25. Fast atom bombardment (FAB) spectra were recorded on a Kratos MS50, using a *meta*-nitrobenzylalcohol or thioglycerol matrix, and accurate mass determinations employed a Kratos Concept IS spectrometer. Microanalyses were performed using a Carlo–Erba 1106 elemental analyser.

Preparation of Polyethyleneglycol Dialdehyde Derivative 2

A solution of oxalyl chloride (0.958 ml, 0.011 mol) in dry dichloromethane (70 ml) under argon was cooled to −60°C. Dimethyl sulfoxide (1.716 ml, 0.0242 mol) was added and after 5 min., polyethyleneglycol **1** (5.00 g, 0.05 mol) was added dropwise over 10 min. at −60°C. After a further 15 min. stirring, 10 ml of anhydrous triethylamine was added dropwise. After 20 min., the mixture was allowed to warm to room temperature and 100 ml of water was added. The aqueous layer was separated and re-extracted with dichloromethane (2 × 100 ml). The combined organic extracts were washed with hydrochloric acid (1 M) (until no longer basic), washed

with water (2 × 50 ml), and saturated sodium chloride solution (2 × 50 ml). The organic extracts were dried and evaporated to give dialdehyde (5.05 g, 99% yield) as a colourless solid; υ_{max} (neat) *inter alia* 1750 (CO), 1110 (CH_2OCH_2) cm^{-1}; δ (^1H, 200 MHz, $CDCl_3$), 3.60 [*m*, $(OC\underline{H}_2C\underline{H}_2)_n$], 4.15(4H, *s*, 2 × $C\underline{H}_2CHO$), 9.70 (2H, *s*, 2 × $C\underline{H}O$).

Preparation of Polyethyleneglycol Ditosylate Derivative

p-Toluenesulfonyl chloride (4.18 g, 0.022 mol) was added to a solution of polyethyleneglycol **1** (10.0 g, 0.10 mol) in triethylamine (40 ml) and the reaction was stirred at room temperature overnight. The mixture was diluted with dichloromethane (30 ml), the white precipitate was removed by filtration, the filtrate was washed with hydrochloric acid (1M, 100 ml), saturated sodium hydrogen carbonate solution (100 ml), dried and evaporated to give the ditosalate (12.23 g, 91% yield) as a colourless solid; δ (^1H, 200 MHz, $CDCl_3$) 2.40 (6H, *s*, 2 × CH_3), 3.40–3.95 [*m*, 2 × $C\underline{H}_2$ $C\underline{H}_2OTs$ and $(OC\underline{H}_2C\underline{H}_2O)_n$], 7.25 and 7.80 (each 4H, *d*, *J* 8Hz, 8 × ArH).

Preparation of Polyethyleneglycol Dibromide Derivative

To a solution of the PEG ditosylate (5.00 g, 0.0037 mol) in Analar acetone (50 ml) was added sodium bromide (0.951 g, 0.00925 mol) and refluxed overnight. The white precipitate was removed by filtration and the acetone solution evaporated to give the dibromide (4.70 g, 96% yield) as colourless solid; δ (^1H, 200 MHz, $CDCl_3$) 3.45 (4H, *t*, *J* 7Hz, 2 × CH_2Br), 3.60 [*m*, $(OC\underline{H}_2C\underline{H}_2O)_n$], 3.80 ($OC\underline{H}_2CH_2Br$).

Preparation of Polyethyleneglycol Dialkene Derivative

Allylmagnesium bromide (41.70 ml, 1.0 M solution in diethyl ether) was added to a solution of polyethyleneglycol dibromide (4.70 g, 0.041 mol) in tetrahydrofuran (30 ml) under argon at −78°C, and stirred at −78°C for 5 h. The reaction mixture was warmed to room temperature and quenched with saturated ammonium chloride. The product was partitioned between ethyl acetate and aqueous ammonium chloride, and the aqueous layer was re-extracted with ethyl acetate (2 × 50 ml). The combined organic extracts were dried and evaporated to give PEG dialkene derivative (5.81 g, 100% yield) as a colourless solid; δ(^1H, 200 MHz, D_2O) 2.65 (4H, quintet, *J* 7Hz, 2 × $OCH_2C\underline{H}_2CH_2$), 2.00–2.15 (4H, *m*, 2 × $OCH_2CH_2C\underline{H}_2$), 3.45 (4H, *t*, *J*7 Hz, 2 × $OC\underline{H}_2CH_2CH_2$), 3.55–3.65 [*m*, $(OC\underline{H}_2C\underline{H}_2)_n$], 4.90–5.05 (4H, *m*,

$2 \times CH{=}\underline{C}H_2$) and 5.65–5.90 (2H, *m*, $2 \times C\underline{H}{=}CH_2$); m/z (f.a.b.) inter alia 1189 (30%, M^++Na), 1145 (50%, M^++Na – OCH_2CH_2), 1101(30%, M^++Na – $2 \times OCH_2CH_2$), 1057 (60%, M^++Na – $3 \times OCH_2CH_2$), 1013 (70%, M^++Na – $4 \times OCH_2CH_2$), 969 (60%, M^++Na – $5 \times OCH_2CH_2$), 925 (60%, M^++Na – $6 \times OCH_2CH_2$), 881(70%, M^++Na – $7 \times OCH_2CH_2$).

Preparation of Polyethyleneglycol Diboronic Acid Derivative 3

Borane tetrahydrofuran (20 ml, 1M solution in tetrahydrofuran) was added to a solution of PEG dialkene derivative (5.00 g, 0.0047 mol) in tetrahydrofuran (40 ml) under argon and refluxed overnight. The reaction was cooled to room temperature and hydrochloric acid added (25 ml, 1M). The product was partitioned between ethyl acetate and the aqueous layer. The aqueous layer was extracted with dichloromethane, and the combined organic extracts were washed with saturated sodium chloride (2×50 ml), dried and concentrated to give diboronic acid **3** derivative (5.73 g, 100% yield); δ(^{11}B, 64.2 MHz, $CDCl_3$) 31.8 [$2 \times CH_2B(OH)_2$]; δ(^{1}H, 200 MHz, $CDCl_3$) 0.60–0.85 [4H, br, $2 \times B(OH)_2$ (disappears upon addition of D_2O)] 0.85–9.95 (4H, *t*, *J* 7Hz, $2 \times CH_2B$), 1.15–1.35 (4H, *m*, $2 \times C\underline{H}_2CH_2B$), 1.30–1.50 (4H, *m*, $2 \times C\underline{H}_2CH_2CH_2B$), 1.45–1.65 (4H, *m*, $2 \times C\underline{H}_2CH_2CH_2CH_2B$), 3.55–3.65 [*m*, $(OC\underline{H}_2C\underline{H}_2)_n$], and 3.70–3.85 (4H, br *t*, *J* 7Hz, $2 \times OC\underline{H}_2CH_2CH_2$).

Preparation of Polyethyleneglycol Diglucamide Derivative 5

A mixture of polyethyleneglycol (PEG) diacid (10.00 g, 0.0166 mol) and thionyl chloride (70.00 ml) were heated under argon, on a steam bath until the evolution of sulfur dioxide ceased. The excess of thionyl chloride was evaporated, and the crude acid chloride was used directly. To a solution of D-glucamide (0.0332 mol, 6.00 g) in tetrahydrofuran (130 ml) and water (20 ml) was added a solution of sodium hydroxide (2M, 30 ml) and the crude PEG diacid chloride simultaneously over a period of 45 min. The pH of the solution was maintained at around approximately 8.0 throughout. The resulting brown solution was evaporated to obtain the crude PEG diglucamide **5** as a brown oil in 99% yield; υ_{max} (neat) *inter alia* 3400 (NH), 1638 (CO) 1100 (CH_2OCH_2) cm^{-1}; δ(^{1}H, 200 MHz, D_2O) 1.15 and 1.19 (each 2H, *s*, $2 \times NHC\underline{H}_2$), 3.00–3.55 and 3.99–4.10 (each 4H, *m*, $8 \times C\underline{H}OH$), and 3.60–3.89 [*m*, $(OC\underline{H}_2C\underline{H}_2)_n$ and $2 \times C\underline{H}_2OH$]; m/z (f.a.b) *inter alia* 928 (30%, M^++H), 884 (100%, $M^+ - OCH_2CH_2$), 840 [60%,

$M^+ - (2 \times OCH_2CH_2)]$, 796 [70%, $M^+ - (3 \times OCH_2CH_2)]$, 752 [70%, $M^+ - (4 \times OCH_2CH_2)]$, 655 [60%, $M^+ + H - (5 \times OCH_2CH_2)]$.

Bottle-test Gel Strength Test: Procedure and Codes

Guar gel samples were prepared by using a Waring blender. 50 ml of the gel was transferred to 40-oz Widemouth Bottles and the bottle was inverted to determine the gel strength code (Tab. IV). The gel preparation experiments were carried out using 500 ml volumes of the guar solution. Most samples were tested using the 50 ml bottle test within 1 day of preparation. There was no appreciable loss of viscosity during this period. There was no addition of any anti-foaming agent; however the solutions generally settled without any problems.

References

[1] Gulbis, J. (1987). 'Fracturing fluid chemistry', *Drilling and Pumping Journal*, Schlumberger Educational Services, Houston, Texas, **7**, 4.
[2] de Gennes, P. G., *Scaling Concepts in Polymer Physics*, Cornell University Press, Ithaca, 1979.
[3] All of the simulations reported in this paper were carried out using the computational chemistry package CERIUS^2, *Molecular Simulations Inc. Version 1.6.* (1995).
[4] Colbourn, E. A. (Ed.), *Computer Simulation of Polymers*, Longman, Harlow, 1994. One favoured way of modelling such molecules is to use the 'united atom' approach, in which typically carbon-hydrogen units along the polymer chain are simulated as single atomic entities. This has the pay-off of enabling MD (and MC) simulations to run much faster.
[5] Brooks, B. R., Bruccoleri, R. E., Olafson, B. D., Sates, D., Swaminathan, S. and Karplus, M. (1983). "Charmm–A program for macromolecular energy, minimization, and dynamics calculations", *J. Comp. Chem.*, **4**,187.
[6] Grootenhuis, P. D. J. and Haasnoot, C. A. G. (1993). *Molecular Simulation*, **10**, 75.
[7] Boek, E. S., Coveney, P. V., Williams, S. J. and Bains, A. S. (1996). "A robust water potential parameterisation", *Mol. Sim.*, **18**, 145.
[8] Aitken, A., Bell, I. S., Coveney, P. V. and Jones, W. (1997). "Simulation of layered double hydroxide intercalates", *Adv. Mater.*, **9**, 496; Bains, A. S., Boek, E. S., Coveney, P. V., Williams, S. J. and Akbar, M. V. (2000). "Molecular modelling of the mechanism of action of organic clay-swelling inhibitors", *Mol. Sim.*, in press.
[9] Mayo, S. L., Olafson, D. and Goddard III, W. A. (1990). *J. Phys. Chem.*, **94**, 8897.
[10] Jorgensen, W. L., Chandrasekhar, J., Madura, J. D., Impey, R. W. and Klein, M. L. (1983). "Comparison of simple potential functions for simulating liquid water", *J. Chem. Phys.*, **79**, 926.
[11] Rothman, D. H. and Zaleski, S. (1994). "Lattice gas cellular automata", *Rev. Mod. Phys.*, **66**, 1417.
[12] Hoogerbrugge, P. J. and Koelman, J. M. V. A. (1992). "Simulating microscopic hydrodynamic phenomena with dissipative particle dynamics", *Europhys. Lett.*, **19**, 155.
[13] Flory, P. J., Statistical Mechanics of Chain Molecules, *Interscience*, New York, 1969.
[14] McCleary, B. and Matheson, N. (1983). *Carbohydrate Res.*, **119**, 191.
[15] Pezron, E. (1990). "Rheology of galactomannan-borax gels", *J. Polymer Sci., Part B*, **28**, 2445.

[16] Donnamaria, M. C., Howard, E. I. and Grigera, J. R. (1994). "Interaction of water with α,α-trehalose in solution-molecular-dynamics simulation approach", *J. Chem. Soc., Faraday Trans.*, **90**, 2731.

[17] Robinson, G., Ross-Murphy, S. B. and Morris, E. R. (1982). "Viscosity molecular-weight relationships, intrinsic chain flexibility and dynamic solution properties of guar galactomannan", *Carbohyd. Res.*, **107**, 17.

[18] Sakurai, Y., US Patent No. 05,262,779. We are grateful to Ray Jasinski for bringing this to our attention. The gel formed presumably occurs due to some degree of borate ester formation. Breakage occurs because glucose forms such strong borate esters, thus scavenging all the boron from the PVA which, with each glucose residue having three hydroxyl groups still left, is water soluble.

[19] In a private communication (1995), Cosgrove informed us of his group's recent work on PEG derivatives in aqueous solution. They have performed Monte Carlo simulations of short chain polymers using Jorgensen's OPLS force field and TIP4P water. They find, like us, that the chains are quite stiff with strong hydrogen bonding to the water solvent molecules. A typical simulation involved the study of molecules such as $CH_3(CH_2)_{11}(OCH_2CH_2)_4$ adsorbed at a water/benzene interface. See, Ito, M. and Cosgrove, T. (1994). "Atomistic simulation of short-chain polymers at the liquid – liquid interface", *Colloids and Surfaces A*, **86**,125. Cosgrove also stated that they estimated a persistance length of 4 Å "based on neutron diffraction using propylene oxides".

[20] Pierleoni, C. and Ryckaert, J.-P. (1992). "Molecular-dynamics investigation of dynamic scaling for dilute polymer-solutions in good solvent conditions", *J. Chem. Phys.*, **96**, 8539.

[21] Schlijper, A. G., Hoogerbrugge, P. J. and Manke, C. W. (1995). "Computer-simulation of dilute polymer-solutions with the dissipative particle dynamics method", *J. Rheol.*, **39**, 567.

[22] Matricardi, P., Dentini, M., Crescenzi, V. and Ross-Murphy, S. B. (1995). "Gelation of chemically cross-linked polygalacturonic acid derivatives", *Carbohyd. Polym.*, **27**, 215.

[23] "Self-aggregation and phase-behavior of poly(ethylene oxide) poly(propylene oxide) poly(ethylene oxide) block-copolymers in aqueous-solution", Almgren, M., Brown, W. and Hvidt, S. (1995). *Colloid Polym. Sci.*, **273**, 2.

[24] "Computer-simulations of a water oil interface in the presence of micelles", Smit, B., Hilbers, P. A. J., Esselink, K., Rupert, L. A. M., van Os, N. M. and Schlijper, A. G. (1990). *Nature*, **348**, 624.